

Archive ouverte UNIGE

https://archive-ouverte.unige.ch

Article scientifique

Article

2004

Published version

Open Access

This is the published version of the publication, made available in accordance with the publisher's policy.

Hollow fiber bioreactor: new development for the study of contrast agent transport into hepatocytes by magnetic resonance imaging

Planchamp Messeiller, Corinne; Ivancevic, Marko Kresimir; Pastor, Catherine; Vallée, Jean-Paul; Pochon, Sibylle Carine; Terrier, François; Mayer, Joaquim; Reist Oechslin, Marianne

How to cite

PLANCHAMP MESSEILLER, Corinne et al. Hollow fiber bioreactor: new development for the study of contrast agent transport into hepatocytes by magnetic resonance imaging. In: Biotechnology and bioengineering, 2004, vol. 85, n° 6, p. 656–665. doi: 10.1002/bit.20017

This publication URL: https://archive-ouverte.unige.ch/unige:42526

Publication DOI: <u>10.1002/bit.20017</u>

© This document is protected by copyright. Please refer to copyright holder(s) for terms of use.

Hollow Fiber Bioreactor: New Development for the Study of Contrast Agent Transport Into Hepatocytes by Magnetic Resonance Imaging

Corinne Planchamp, Marko K. Ivancevic, Catherine M. Pastor, Sibylle Pochon, François Terrier, Joachim M. Mayer, Marianne Reist

¹Geneva University Hospital, Radiology Department, Micheli-du-Crest 24, CH-1211 Geneva 14, Switzerland; telephone: +41 22 372 93 53; fax: +41 22 372 93 66; e-mail: corinne.planchamp@hcuge.ch
²Bracco Research SA, Geneva, Switzerland
³University of Lausanne, School of Pharmacy, Lausanne, Switzerland

Received 6 June 2003; accepted 19 November 2003

Published online 30 January 2004 in Wiley InterScience (www.interscience.wiley.com). DOI: 10.1002/bit.20017

Abstract: The aim of our study was to develop a magnetic resonance (MR)-compatible in vitro model containing freshly isolated rat hepatocytes to study the transport of hepatobiliary contrast agents (CA) by MR imaging (MRI). We set up a perfusion system including a perfusion circuit, a heating device, an oxygenator, and a hollow fiber bioreactor (HFB). The role of the porosity and surface of the hollow fiber (HF) as well as the perfusate flow rate applied on the diffusion of CAs and O₂ was determined. Hepatocytes were isolated and injected in the extracapillary space of the HFB $(4 \times 10^7 \text{ cells/mL})$. The hepatocyte HFB was perfused with an extracellular CA, gadopentetate dimeglumine (Gd-DTPA), and gadobenate dimeglumine (Gd-BOPTA), which also enters into hepatocytes. The HFB was imaged in the MR room using a dynamic T_1 -weighed sequence. No adsorption of CAs was detected in the perfusion system without hepatocytes. The use of a membrane with a high porosity (0.5 µm) and surface (420 cm²), and a high flow rate perfusion (100 mL/min) resulted in a rapid filling of the HFB with CAs. The cellular viability of hepatocytes in the HFB was greater than 85% and the O2 consumption was maintained over the experimental period. The kinetics of MR signal intensity (SI) clearly showed the different behavior of Gd-BOPTA that enters into hepatocytes and Gd-DTPA that remains extracellular. Thus, these results show that our newly developed in vitro model is an interesting tool to investigate the transport kinetics of hepatobiliary CAs by measuring the MR SI over time. © 2004 Wiley Periodicals, Inc. Keywords: hollow fiber bioreactor; magnetic resonance imaging; contrast agent; hepatocyte; Gd-BOPTA; transport

INTRODUCTION

Magnetic resonance imaging (MRI) is a noninvasive and safe method for the detection and characterization of diseases in

Correspondence to: Corinne Planchamp

Contract grant sponsor: Fonds National Suisse de la Recherche Scientifique

Contract grant number: N 3200-100 868 (to C.M.P.)

the entire body. In patients, the injection of contrast agents (CAs) during MRI increases the detection of hepatic focal lesions and better characterizes diffuse diseases (Hahn and Saini, 1998; Semelka and Helmberger, 2001; Taylor and Ros, 1998). The most commonly used CAs are the nonspecific extracellular gadolinium chelates such as gadopentetate dimeglumine (Gd-DTPA) because they are inexpensive, safe, well-tolerated, and detect a wide range of hepatic diseases. New CAs that are selectively taken up by hepatocytes, such as gadobenate dimeglumine (Gd-BOPTA) or mangafodipir trisodium (Mn-DPDP), have been recently developed. These CAs are taken up specifically by hepatocytes and are partially excreted into the bile. This category of CAs enhance the signal intensity (SI) on T_1 weighted images in tissues which possess specific transporters. Normal livers and focal hepatic lesions containing functional hepatocytes take up these agents.

Nonspecific extracellular gadolinium chelates remain extracellular and do not enter hepatic cells. After i.v. injection, plasma Gd-DTPA concentration rapidly declines, with a rapid distribution into the vascular compartment. In the liver, the agent diffuses exclusively in the extracellular space. The hepatocyte uptake and bile excretion of the agent are negligible and the overall body excretion of the drug occurs by glomerular filtration. In contrast, following an i.v. injection, Gd-BOPTA distributes into the extracellular space and then enters into hepatocytes (De Haën et al., 1999). This agent is highly water soluble, exhibits low plasma protein binding and is not metabolized (Lorusso et al., 1999). It is eliminated via both the renal and biliary routes. Gd-BOPTA is likely to enter into hepatocytes via transporters localized on the sinusoidal membrane but the mechanisms responsible for the hepatocyte uptake of this CA are incompletely known. The excretion of Gd-BOPTA into the bile occurs via the multidrug resistance-associated protein Mrp2 located at the canalicular side of hepatocytes (De Haën et al., 1996, 1999; Pascolo et al., 2001).

In vitro cellular models are of great value for the study of such transport mechanisms. Hollow fiber bioreactors (HFBs) imitate the in vivo situation by interposing a semipermeable membrane between the circulating solution and the cell mass. This perfusion solution supplies cells with O₂ and nutrients and removes the metabolic products. Under these approximately physiological conditions, cellular functions are maintained. For these reasons, HFB with mammalian cells are used in biotechnology for the production of mammalian cell-derived products such as antibodies (Jackson et al., 1996; Kreutz et al., 1997) or hormones (Knazek and Skyler, 1976; Liu et al., 1991) and for the development of artificial organs such as pancreas (Tze et al., 1980) or liver (Allen et al., 2001; Patzer, 2001).

The aim of our study was to develop an MR-compatible HFB containing freshly isolated rat hepatocytes in order to study the transport kinetics of Gd-BOPTA into hepatocytes. The role of the porosity and surface of the HF as well as the perfusate flow rate applied on the diffusion of CAs and O₂ was determined. Kinetics of Gd-DTPA (extracellular CA) and Gd-BOPTA (which also enters into hepatocytes) were studied by imaging the HFB containing hepatocytes in the MR unit.

MATERIALS AND METHODS

Chemicals

Gd-BOPTA was provided by Bracco Research (Geneva, Switzerland). Gd-DTPA is commercially available (Mag-

nevist, Schering, Germany). Bovine serum albumin (BSA, fraction V, 97%) and ethyleneglycol-O,O'-bis(2-amino-ethyl)-N,N,N',N'-tetraacetic acid (EGTA) were purchased from Fluka (Buchs, Switzerland). Collagenase from *Clostridium histolicum* type IV (collagen digestion activity: 295 U/mg solid) and bovine pancreas insulin were obtained from Sigma Chemical (St. Louis, MO). All other chemicals were of analytical grade.

MR-Compatible Perfusion System

The MR-compatible perfusion system included a closed perfusion circuit, a heating device (Fig. 1, D and H), an oxygenator (I), a bubble trap (J), and an HFB (K).

To avoid interference with the magnetic field, all material used in the MR unit was free of metal and made of plastic and glass. The heating device, the O₂-CO₂ tank (B), and the pump (C) were installed in an adjacent room. All elements inside the magnet were fixed to a PVC support built to fix the HFB at the isocenter of the magnet.

Perfusion Circuit

The perfusion circuit included two reservoirs (A) containing the different solutions to be perfused during the experiment. These reservoirs were connected to the HFB by long (15 m) tubing (Tygon 2257, ID 1/8′, OD 3/16′, and Pharmed 65, ID 1/4′, OD 3/8′, Saint-Gobain Performance Plastics, Akron, OH). This tubing was chosen to minimize the adsorption of CA. The solution flowed from the reservoir to the HFB by a peristaltic pump. To avoid the entry of gas bubbles into the

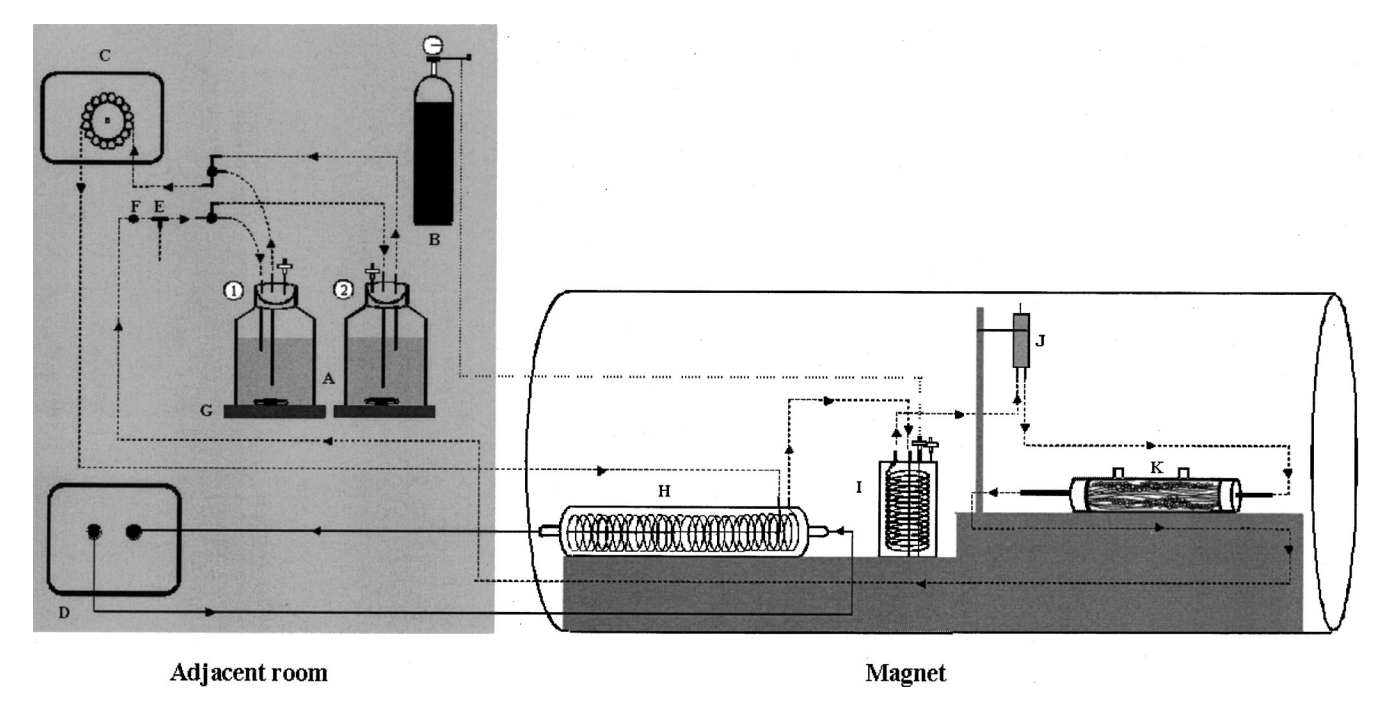


Figure 1. Schematic drawing of the hollow fiber bioreactor perfusion system. The system was composed of solution reservoirs 1 and 2 (A), a gas bottle (B), a peristaltic pump (C), a heating circulator (D), a sampling port (E), a temperature probe (F), a magnetic stirrer (G), a glass spiral (H), an oxygenator (I), a bubble trap (J), and a hollow fiber bioreactor (K). Elements A to G were placed in a room adjacent to the magnet room.

HFB, a plastic bubble trap was installed just before its inlet. A port allowed sampling for analysis.

Heating System

The solutions of perfusion were heated by circulating a refrigerant through a glass spiral (Fig. 1, H) while hot water flowed outside the spiral. Hot water was provided by the thermostatic bath (Haake N6, Karlsruhe, Germany) (D) placed outside the MR unit. The refrigerant was installed in the magnet, just before the oxygenator system. Tubing (15 m) was connected between the bath and the glass spiral in the magnet. Temperature measurements were made using a thermocouple thermometer (Extech Instruments, no. 422315, Waltham, MA). To avoid interference with the magnetic signal, the temperature probe (F) was placed at the outlet of the HFB near the solution reservoirs.

Oxygenator

Oxygenation of isolated hepatocytes was obtained by flowing the solution of perfusion in a thin-walled silicone tubing (Silastic, ID 0.132′, OD 0.183′, Dow Corning, Midland, MI) permeable to O₂ and CO₂. Tubing (7 m) was coiled in a plastic box (Hamilton et al., 1974). A tank (95% O₂/5% CO₂) was connected to the oxygenator to obtain high pO₂ (>50 kPa) and normal pCO₂ (5 kPa).

Hollow Fiber Bioreactor

The HFB consisted of a network of semipermeable artificial capillaries bundled together within a transparent plastic shell. The perfusion solution was pumped from the reservoir, oxygenated and heated, and flowed within the intracapillary space (ICS) before diffusing through the semipermeable membrane into the extracapillary space (ECS). The HFBs used (Minikros Sampler, Spectrum, Rancho Dominguez, Houston, TX) were made of hydrophilic polyethersulfone fibers (0.5 mm diameter). The ECS and ICS volumes were respectively 25 mL and 5 mL. Various modules were tested with various fiber surface area (FSA) and porosity. Module 1 (product no. M15E 220 01N) had an FSA of 140 cm² and a porosity of 0.5 µm; module 2 (product no. M15E 260 01N) had an FSA of 420 cm² and a porosity of 0.5 µm; module 3 (product no. M12E 220 01N) had an FSA of 140 cm² and a porosity of 0.2 μm. During perfusion, the HFB was surrounded by an Armaflex jacket for thermal insulation.

Hepatocyte Hollow Fiber Bioreactor

Animals

Adult male Sprague-Dawley rats (250–350 g) were purchased from Charles River Laboratory (Iffa Credo, L'Arbresle, France). Rats were housed in standard cages in a temperature-controlled room (21–25°C) with a 12-h light/

dark cycle. Standard laboratory chow and water were given ad libitum. The protocol was approved by our local veterinary office.

Isolation of Hepatocytes

Hepatocytes were isolated by a two-step collagenase perfusion of the liver as described by Seglen (1976). Briefly, after rat anesthesia (i.p., sodium pentobarbital, 80 mg/kg), a midline incision was performed and the portal vein was cannulated. Then the liver was perfused with a buffer solution containing 0.50 mM EGTA, at 37°C with a 30 mL/min flow rate. After 10 min, collagenase (0.05%) and CaCl₂ (2.00 mM) were added to the buffer solution (pH 7.55) and the solution was perfused for 10 min. Buffer solution included 151 mM NaCl, 5.37 mM KCl, 0.63 mM Na₂HPO₄, 0.44 mM KH₂PO₄, 4.2 mM NaHCO₃, and 5.55 mM glucose.

After collagenase perfusion, the liver was removed and transferred to a cold buffer solution containing 0.5% BSA and 0.41 mM MgSO₄, pH 7.4. The hepatocytes were gently released by shaking after disruption of the Glisson capsule. Cell suspension was filtered (100 µm nylon mesh) and the viable cells were allowed to sediment. The supernatant containing debris and dead cells was discarded. With this technique, cell viability was greater than 90% (Trypan blue exclusion). An average of 5×10^8 cells were isolated from a single liver. Cells were washed with the buffer solution. The cells in solution were centrifuged (550 rpm, 50 g, 2 min, 4°C) and the remaining cell pellet was suspended in ice-cold modified University of Wisconsin (UW) solution (30 mL) containing 80 mM lactobionic acid, 30 mM raffinose, 25 mM KH₂PO₄, 25 mM NaOH, 10 mM glycine, 5 mM MgSO₄, 5 mM adenosine, 1 mM allopurinol, 165700 U/l Penicillin G, 5% PEG 800, and 0.5% BSA. The pH of the solution was adjusted to 7.4 with 2.5 N KOH (~55 mM). The UW solution was aseptically filtered before use (Millex GS, 0.22 µm, Millipore, Bedford, MA). The suspension was kept at 4°C before loading in the bioreactor. Hepatocytes preserved at 4°C in this solution remain functional and viable for several hours without deterioration of transport functions (Hammond and Fry, 1993; Olinga et al., 1997; Sandker et al., 1990, 1992).

Hepatocyte Loading Into the Bioreactor

The HFB was rinsed with distilled water (1 L) in a single pass through the fibers at 50 mL/min. The HFB was then autoclaved by a 30-min cycle at 121°C. Just before the cell loading, the ECS and ICS of the HFB were flushed with UW solution, taking care not to introduce air bubbles. The hepatocytes suspended in UW solution were centrifuged (550 rpm, 50 g, 5 min, 4°C) and the pellet was injected into the ECS of the HFB. Hepatocytes were gently poured in a sterile 50 mL luer-lock syringe without piston fixed at an ECS port. Cells were aspirated into the ECS by another syringe fixed at the second ECS port. The bioreactor was preserved at 4°C for up to 4 h until experiment.

Hepatocyte Viability

During the experiments the cell viability was checked by measuring lactate dehydrogenase (LDH) and aspartate aminotransferase (AST) release in the perfusate (Roche Diagnostics, Rotkreuz, Switzerland) and by determining the hepatocyte O₂ consumption using a blood gas analyzer (ABL 500, Radiometer Copenhagen, Brunson, DK).

LDH and AST release was expressed as a percentage of the total concentration of LDH and AST contained in hepatocytes. Intracellular LDH and AST after cellular lysis with Triton X-100 was measured (Mamprin et al., 1995). Briefly, freshly isolated hepatocyte suspension (0.5 mL, 5×10^6 cells) were added to a Triton X-100 solution 0.1% (9.5 mL) and mixed for 1 h. The mixture was centrifuged (10000 rpm, 400g, 4 min) and LDH and AST concentration in the supernatant were measured.

To calculate the O_2 consumption of hepatocytes in the bioreactor, buffer samples were collected before and after the HFB and analyzed off-line immediately. The hepatocyte O_2 consumption (ΔO_2) was determined with the following equation (Nyberg et al., 1994):

$$\Delta O_2 = S(O_2) \times [P_{in} - P_{out}] \times Q_E$$
 (1)

where P_{in} and P_{out} are the O_2 tensions (kPa) before and after the HFB, Q_E is the flow rate (mL/h), and $S(O_2)$ is the O_2 solubility in water at 37°C (9.68 × 10⁻⁶ mol O_2 /mL/kPa).

HFB Perfusion

The HFB circuit was filled with the following perfusion solution: 76.0 m*M* NaCl, 5.37 m*M* KCl, 0.63 m*M* Na₂HPO₄, 0.44 m*M* KH₂PO₄, 17.9 m*M* NaHCO₃, 2.00 m*M* CaCl₂, 0.41 m*M* MgSO₄, 40.0 m*M* HEPES Na, 5.55 m*M* glucose, 99420 U/L Penicillin G, 77700 U/L streptomycin sulfate, 280 U/L insulin, and 0.5% BSA. Perfusion solutions were aseptically filtered before use (Millex GP₅₀, 0.22 μm, Millipore) and kept at 4°C in sterile glass bottles. The first 50 mL was discarded to eliminate residual distilled water. Then the solution was recirculated and warmed until the required temperature was obtained (36.5°). At that time the HFB was introduced into the circuit.

Magnetic Resonance Imaging

The HFB was imaged by a dynamic T_1 -weighted sequence using fast gradient echo sequence FAST (Gyngell, 1988; Ivancevic et al., 2001) with the following imaging parameters: $90-180^{\circ}$ magnetization preparation, TI/TR/TE 28/10.52/4 msec, FA 90° , FOV 10 cm, matrix size 256×256 , slice thickness 5 mm. The interimage delay was 2.5 sec during the determination of the HF module to be chosen and 20 sec for all other experiments.

During perfusion, eight cross sections through the HFB inlet tubing, reference vials containing 0.5, 2, and 4 m*M* of Gd-DTPA, and the HFB were imaged on an Eclipse 1.5 T MR system (Marconi Medical Systems, Cleveland, OH) us-

ing a wrist coil (Fig. 2). Results are expressed as the mean SI in a central cross-section over time normalized to the SI obtained in the 4-mM reference vial and the baseline value.

To increase the resolution, a high-resolution image was obtained after each perfusion by a spin echo sequence with the following imaging parameters: TR/TE 400/20 ms, bandwidth 20.83 kHz, slice thickness 5 mm, matrix size 512×512 , number of averages 2, slices 8.

Experimental Protocol

Determination of a Potential Adsorption of CAs in the Perfusion System

To investigate a potential adsorption of CAs in the perfusion system, Gd-BOPTA and Gd-DTPA solutions (0.2 m*M*) were circulated through the system (100 mL/min, 37°) for 240 min and the UV absorbance of the perfusion solutions was regularly measured at the maximal wavelength of the CA (210 or 190 nm, respectively) with a UV spectrophotometer (1601, Shimadzu, Kyoto, Japan). For comparison, the adsorption of 7-ethoxycoumarin (7-EC) was studied under the same conditions by circulating buffer + 7-EC (0.015 m*M*) through the perfusion system. Perfusate samples were analyzed by fluorimetry (LS 50 B, Perkin Elmer, Norwalk, CT) at the maximal wavelengths of excitation and emission of 7-EC (333 nm and 394 nm, respectively).

Optimization of the System

The optimization of the system was made by determining the best porosity and surface of the HF as well as the best flow rate applied to allow rapid and high diffusion of CAs and consequently of nutrients and O_2 from the ICS into the ECS. The best hepatocyte density was also investigated. This density should be high enough to permit MR detection of cellular effects without side effects on cell viability.

To choose the best HFB, the circuit with the HFB and no hepatocyte was introduced in the magnet and perfused with

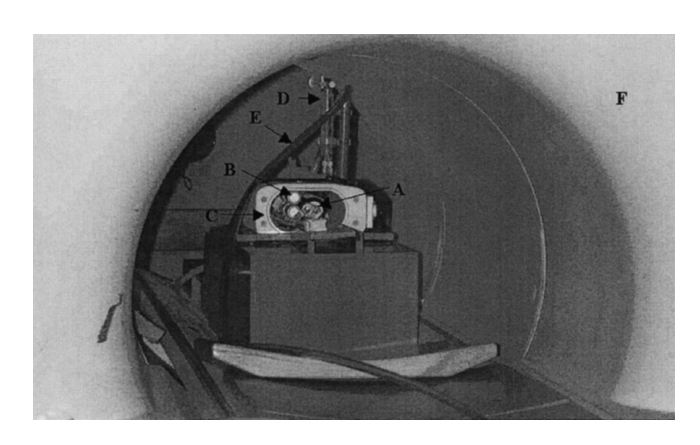


Figure 2. MR part of the perfusion system. The hollow fiber bioreactor with hepatocytes (A), was surrounded by reference vials (B), wrist coil (C), bubble trap (D), and the oxygen-delivering tubing (E). The whole system was placed in the MR magnet (F).

2 mM Gd-DTPA at 100 mL/min. Three HFB modules were tested by perfusing the system with the buffer solution (15 sec) and then the buffer + 2 mM Gd-DTPA solution (5 min).

To determine the optimal flow rate, similar experiments were performed with buffer + 0.2 mM Gd-DTPA solution at 50, 75, and 100 mL/min. The HFB module used was the one determined in the previous experiment.

To model the kinetics of filling, MR SI over time measured in an HFB cross-section were submitted to compartmental analysis using the software MicroPharm (v. 4.0, 1995, Inserm, France). Equation (2) describes the one-compartment model while the two-compartment model is described by Eq. (3) (A and B: proportionality constants, k, k_1 and k_2 : transfer rate constants, t: time).

$$SI = A \cdot [1 - e^{-k \cdot t}] \tag{2}$$

$$SI = A \cdot [1 - e^{-k_1 \cdot t}] + B \cdot [1 - e^{-k_2 \cdot t}] \tag{3} \label{eq:3}$$

The relationship between the rate constant (k) and the half-life $(t_{1/2})$ is given by Eq. (4):

$$t_{1/2} = \frac{\ln 2}{k} \tag{4}$$

To determine the adequate cell density to introduce into the HFB, cell viability was tested with two different densities outside the MR unit. HFB were loaded with hepatocytes at densities of 2×10^7 (total number of cells: 0.5×10^9) and 4×10^7 cells/mL (total number of cells: 1×10^9). The HFBs were perfused for 4 h with a buffer at 100 mL/min. LDH and AST concentrations in the perfusate were measured every hour.

Imaging of the HFB With Hepatocytes

The system was perfused with buffer (30 min), buffer + Gd-DTPA (0.2 mM, 20 min), buffer (20 min), buffer + Gd-BOPTA (0.1 and 0.2 mM, 30 min), and buffer (30 min). For these experiments the optimal HFB module, flow rate, and

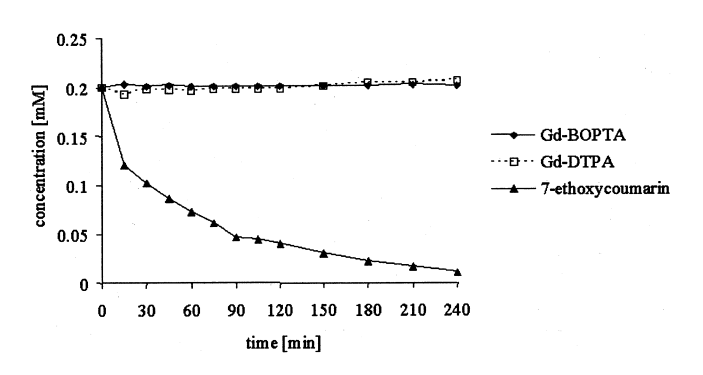


Figure 3. Gd-BOPTA, Gd-DTPA, and 7-ethoxycoumarin (7-EC) concentrations in the perfusion solution over time. The hollow fiber bioreactor was perfused for 240 min in the absence of hepatocytes. Gd-BOPTA and Gd-DTPA were measured by UV absorbance and 7-EC by fluorimetry.

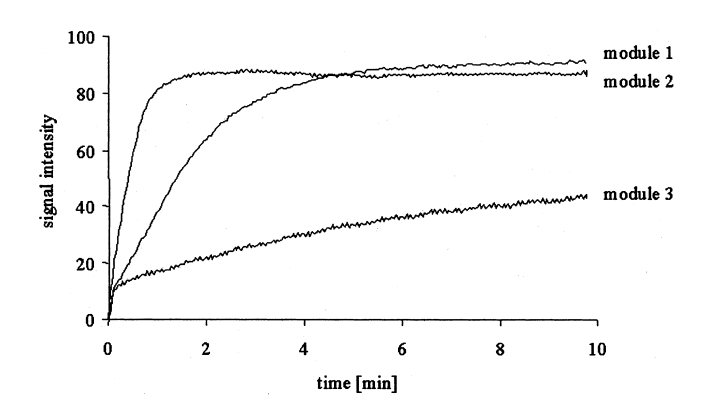


Figure 4. MR signal intensity during the perfusion of hollow fiber bioreactors (HFBs) with Gd-DTPA over time: influence of the fiber surface area (FSA) and porosity of the fibers. Module 1: porosity = $0.5 \, \mu m$, FSA = $140 \, cm^2$; module 2: porosity = $0.5 \, \mu m$, FSA = $420 \, cm^2$; module 3: porosity = $0.2 \, \mu m$, FSA = $140 \, cm^2$. The HFBs without hepatocytes were perfused with a buffer solution (15 sec) and 2 mM Gd-DTPA (10 min). Flow rate = $100 \, mL/min$.

cell density determined in the previous experiments were chosen. A control experiment without hepatocytes in the HFB was performed under the same conditions to exclude unspecific adsorption of the CAs on the surface of the bioreactor capillaries.

At the end of the experiments, cells were extracted from the bioreactor and lysed with Triton X-100 (0.1% solution). The mixture was centrifuged, the supernatant collected, and analyzed by inductively coupled plasma atomic emission spectrometry (ICP-AES) to determine the gadolinium content and thereby the intracellular retention of CA.

RESULTS

Gd-BOPTA and Gd-DTPA Are Not Adsorbed in the Perfusion System

When Gd-BOPTA and Gd-DTPA were perfused in the system without hepatocytes, the concentrations of the two

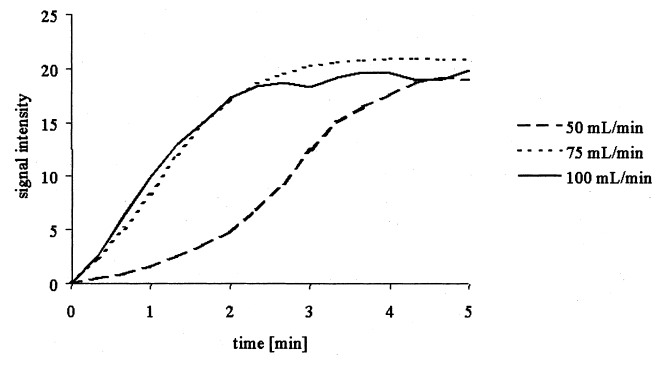


Figure 5. MR signal intensity during the perfusion of hollow fiber bioreactors (HFBs) with Gd-DTPA over time: influence of the flow rate. The HFBs without hepatocytes were perfused with a buffer solution (15 sec) and 0.2 mM Gd-DTPA (5 min). Three flow rates were tested (50, 75, and 100 mL/min).

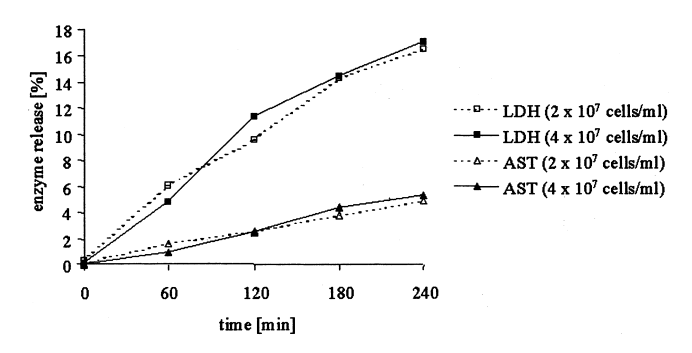


Figure 6. Hepatocyte viability in the hollow fiber bioreactors (HFBs): influence of cell density. The HFBs were perfused with buffer for 240 min and the LDH and AST release in the perfusate was measured over time. Two cell densities were tested $(2 \times 10^7 \text{ and } 4 \times 10^7 \text{ cells/mL})$. LDH and AST release was expressed as a percentage of the total concentration of AST and LDH contained in hepatocytes.

CAs were not modified over time (Fig. 3). In contrast, the concentration of 7-EC decreased over time, and most of the product was adsorbed in the oxygenator tubing.

Determination of the Best HFB

Diffusion of Gd-DTPA (2 mM) into the ECS of HFB with fibers of various surface area and porosity was studied in the MR unit. During these experiments, the flow rate was 100 mL/min. A steady-state was rapidly reached with modules 1 and 2 (Fig. 4). Because the porosity in these two modules was 0.5 μm (0.2 μm for module 3), the higher the porosity of the fibers, the faster the achievement of a steady-state. Diffusion was more rapid when the FSA was 420 cm² (module 2). Filling of modules 1 and 2 was fitted successfully with a one-compartment model. Half-lives were 0.3 (420 cm²) and 1.3 min (140 cm²). Filling of module 3 was consistent with a two-compartment model. Half-lives were 0.1 (phase 1) and 4.6 min (phase 2). Consequently, module 2 was chosen for the following experiments.

Determination of the Optimal Flow Rate

To achieve a rapid and high diffusion rate into the ECS, various flow rates were tested in the HFB without hepatocytes. The SI measured by MRI during Gd-DTPA perfusion was tested at 50, 75, and 100 mL/min. A steady-state was obtained with the three flow rates tested, but the

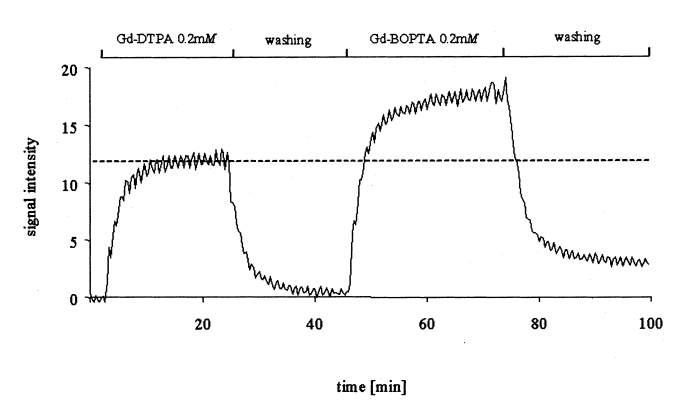


Figure 7. Representative drawing of MR signal intensity during the perfusion of Gd-DTPA and Gd-BOPTA in the hollow fiber bioreactor (HFB) with 4×10^7 hepatocytes/mL. The HFB was perfused with buffer, 0.2 mM Gd-DTPA (20 min), buffer (20 min), 0.2 mM Gd-BOPTA (30 min), and finally buffer (30 min). Dashed line indicates the maximal SI obtained with the extracellular contrast agent Gd-DTPA.

velocity differed with the flow rate (Fig. 5). A steady-state was obtained rapidly with both 75 and 100 mL/min, but the diffusion of Gd-DTPA in the ECS was slower at 50 mL/min. The kinetic analysis enabled measurement of the diffusion difference between flow rates of 75 and 100 mL/min. The kinetic analysis of the SI over time showed that the diffusion was described with a one-compartment model, with half-lives of 1.00 \pm 0.05 (75 mL/min) and 0.82 \pm 0.04 min (100 mL/min). Therefore, the 100 mL/min was chosen for the subsequent experiments.

Adequate Hepatocyte Density in the HFB

To determine the adequate hepatocyte density in the HFB in order to obtain the best SI without hepatocyte damage, two densities $(2 \times 10^7 \text{ and } 4 \times 10^7 \text{ cells/mL})$ were tested in our system. Because LDH and AST release were identical with the two densities chosen and indicated that cell viability was greater than 83% after 4 h of perfusion (release <17%) (Fig. 6), a density of 4×10^7 cells/mL was selected for the following experiments.

Imaging of the HFB With Hepatocytes

Kinetics of the extracellular CA (Gd-DTPA) and the CA which enters into hepatocytes (Gd-BOPTA) were finally

Table I. Range of signal intensity (SI) measured during perfusion with Gd-DTPA and Gd-BOPTA and after washing.

	0.2 m M Gd-DTPA (min - max, $n = 3$)	0.2 mM Gd-BOPTA (min - max, $n = 3$)	0.1 m M Gd-BOPTA (min - max, $n = 3$)
Maximal SI during perfusion SI after washing	11.9-12.2	15.1-17.1	7.4-10.4
	0.1-0.5	1.7-3.0	1.2-1.5

SI were normalized (reference vial $4~\mathrm{m}M$) and corrected for baseline value.

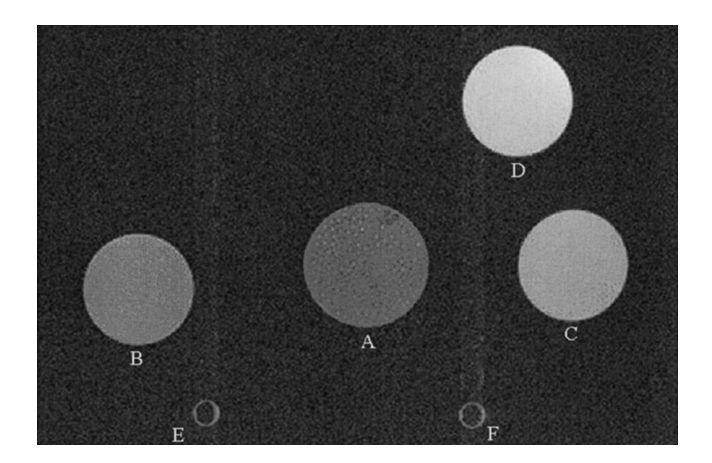


Figure 8. Imaging of the hollow fiber bioreactor (HFB) containing hepatocytes. The system was imaged by a spin echo sequence (TR/TE 400/20 ms, bandwidth 20.83 kHz, slice thickness 5 mm, matrix size 512×512). HFB (A), was surrounded by three reference vials containing 0.5 (B), 2 (C), and 4 mM (D) Gd-DTPA, and by HFB inlet (E) and outlet tubing (F). The hollow fibers and hepatocytes are easily observed in the HFB (A).

tested in our system. During the perfusion of Gd-DTPA, the SI rapidly increased and reached a steady-state (Fig. 7). The SI returned to baseline during the washing. During the perfusion of Gd-BOPTA, the SI increased rapidly and then more slowly, without reaching a steady-state. During the washing, the SI decreased rapidly but remained at a higher value than that observed after Gd-DTPA. The SI never returned to the baseline while in similar experiments performed without hepatocytes, the SI always returned to the baseline after the washing of both CAs.

The SI measured at the end of the perfusion and at the end of the washing was higher for 0.2 mM Gd-BOPTA than for 0.2 mM Gd-DTPA (Table I). Moreover, the SI measured at the end of the perfusion and at the end of the washing was higher after 0.2 mM Gd-BOPTA perfusion than after 0.1 mM Gd-BOPTA perfusion. The amount of Gd-BOPTA contained in the hepatocytes after perfusion with 0.2 mM Gd-BOPTA and washing was 57.8 \pm 4.8 μ g/ 10^9 cells (n = 3) as determined by ICP-AES.

During the CA perfusion the cell viability was tested. The O_2 consumption was $663 \pm 52 \,\mu\text{M/h}$ during the first hour and then increased to $1{,}037 \pm 27 \,\mu\text{M/h}$. At the end of the protocols the cell viability was routinely greater than 85%, based on the amount of AST and LDH released in the perfusate (<15%).

The HFs were well defined by the high-resolution image of the HFB (Fig. 8). Space outside the HF was homogeneous, suggesting a uniform distribution of hepatocyte in the ECS.

DISCUSSION

MR-Compatible HFB

Methods used for CA detection in in vitro cellular models include radioactivity measurements of radiolabeled CAs (Gallez et al., 1996b; Pascolo et al., 1999; Van Montfoort

et al., 1999) and fluorescence for iron oxide particle-based CAs (Reimer et al., 1998; Schulze et al., 1995). ³¹P magnetic resonance spectroscopy (MRS) is also applied for the quantification of Mn-DPDP (Colet et al., 1998; Gallez et al., 1996a). The use of MRI as an analytical tool for the study and quantification of CAs in vitro is limited because of the low MRI spatial resolution achievable in cultured cells with the currently available MR systems. Consequently, MRI detection of CAs in isolated cells requires a high cell density. Moreover, the impossibility of using metallic devices inside the magnet complicates the use of tissue or cell cultures which require controlled temperature and oxygenation. However, the advantage of MRI over the other quantification techniques is that all kinds of MRI CAs can be tested without the need of radiolabeled molecules.

HF systems with mammalian cells have been developed to mimic the in vivo environment. They have been used with various cell types to synthesize cellular products. They have also been tested as bioartificial organs to replace failing organs. The high cell density obtained in HFBs is the major advantage cited by Gillies et al. (1991), who pioneered an MR-compatible HFB system containing hybridoma cultures. Other authors used MRS/MRI techniques to test the performance of HFBs containing mammalian cells (Donoghue et al., 1992; Potter et al., 1998) and bioartificial livers (Macdonald et al., 1998). Others used these techniques to characterize the flow distribution in HFBs without cells (Hammer et al., 1990; Osuga et al., 1998; Zhang et al., 1995). However, to our knowledge, the only cell cultures which have been used to quantify the cellular transport of CAs by MRI are static cell cultures, such as cell pellets and cell monolayers (Aime et al., 2002; Schmalbrock et al., 2001). Although more difficult to set up, we developed a hepatocyte HFB to study the transport of CAs by MRI because, in addition to optimal hepatocyte oxygenation and consequently excellent viability, it permits measurement of CA kinetics as achieved in patients. For these reasons, our HFB is an interesting and innovative approach.

Setup of the MR-Compatible HFB

Adequate oxygenation of perfusion solution was ensured by the use of a silicone membrane highly permeable to $\rm O_2$ and $\rm CO_2$ similar to the one first described by Knazek et al. (1972). When using silicone, one must be aware of possible adsorption of solutes by the tubing. No adsorption of Gd-DTPA nor Gd-BOPTA was detected in our perfusion system, in contrast to 7-EC, which was almost completely adsorbed to the system (Fig. 3). Other substances like antibiotics (Mizutani, 1982) or fentanyl (Rosen et al., 1990) were reported to adsorb on silicone tubing.

We tested three modules available in the market according to the following criteria: 1) large fiber porosity and surface to maximize exchange between the ICS and the ECS with rapid CA concentration equilibrium and optimal oxygenation and nutrients to hepatocytes; 2) large diameter for the HFB to allow MRI analysis; and 3) small volume to concentrate

cells. The three modules tested had the same dimensions but differed by the HF surface and porosity. Comparison of modules with the same FSA (140 cm²) showed the influence of the porosity on the filling: the higher the porosity (0.5 μ m vs. 0.2 μ m) the faster the achievement of a steady-state. The influence of the FSA was obvious in modules with similar porosity (0.5 μ m,): the higher the FSA (420 cm² vs. 140 cm²) the faster the filling (Fig. 4).

Compartmental kinetic analysis enabled quantification of the filling of the HFB with CA. The filling process of modules 1 and 2 was described successfully with a one-compartment model, while a two-compartment model described the filling of module 3. These results suggest that with modules 1 and 2 both the fiber filling with Gd-DTPA and the diffusion through the fibers in the ECS were too rapid to be distinguishable. In contrast with module 3, the first phase, characterized by a short half-life, probably corresponded to the filling of the hollow fibers with Gd-DTPA and the second phase, characterized by a long half-life, corresponded to the diffusion of CA through the fibers in the ECS and was the rate-limiting step. Because the steady-state was reached with the shortest time period, module 2 was chosen for subsequent experiments.

A fast diffusion of CA into the ECS was achieved with the highest flow rate tested (100 mL/min) (Fig. 5). The higher rate of solute appearance in the ECS with increased flow rate has been reported by others (Giorgio et al., 1993; Rozga et al., 1993). Increasing the flow rate over 100 mL/min would not have changed the diffusion rate (which was stable between 75 and 100 mL) but could have improved O₂ and nutrient delivery to the hepatocytes. However, a high flow rate can increase cell shear stress when hepatocytes are present in the HFB, which might be prejudicial to cell viability (Tharakan, 1986). Thus, a compromise between optimal diffusion, adequate oxygenation, and minimal cell shear stress was made and the flow rate was fixed at 100 mL/min.

Finally, the use of the HFB with the biggest porosity and surface area together with a high flow rate resulted in a rapid concentration equilibrium between the ICS and the ECS of the bioreactor. Rapid and total diffusion of CAs was very important, as the aim of the study was to investigate transport into hepatocytes. Rapid diffusion of O_2 and other nutrients is also crucial for the maintenance of hepatocyte viability.

A high hepatocyte density in the HFB is important to allow SI detection by MRI. Moreover, oxygenation must be sufficient to maintain cell function and viability during the experiment. Two different cellular densities were compared: 2×10^7 (hepatocytes isolated from a single rat liver) and 4×10^7 cells/mL (hepatocytes isolated from two rat livers). According to the literature, hepatocyte density is assumed to be about 10^8 cells/mL in the liver (Greengard et al., 1972; Sasse et al., 1992; Weibel et al., 1969). Hence, the higher density tested in our system corresponded to 40% of the density found in vivo. With this density, oxygenation was adequate as assessed by cell viability measurements (AST and LDH release <17%). A higher density was not tested because 4×10^7 cells/mL was sufficient to detect MR SI.

Interestingly, the high-resolution image of the hepatocyte HFB showed a homogeneous distribution of hepatocytes in the ECS (Fig. 8).

Hepatocyte Viability in the HFB

Using AST and LDH release as a cellular viability marker, the viability of hepatocytes was greater than 85% after a 3-h perfusion. During the experiment, the O_2 consumption increased from $\sim 700~\mu\text{M/h}$ to $\sim 1,000~\mu\text{M/h}$. This increase may be explained by the rewarming of the cells (from $4-37\,^{\circ}\text{C}$) at the initiation of the perfusion. The cellular activity, reflected by the O_2 consumption, may progressively increase when the temperature rises. For this reason, the hepatocyte HFB is perfused for 30 min with buffer before the CA perfusion. As the temperature is difficult to maintain at a steady-state, PO_2 may parallel the temperature change. The use of an O_2 probe in the circuit allowing continuous measurements may avoid this problem (Gamcsik et al., 1995).

The O_2 consumption we obtained in our system is in good agreement with that obtained by Rotem et al. (1992), who studied the O_2 consumption of hepatocytes seeded on collagen gels. In this study, the O_2 consumption was $1490 \,\mu\text{M/h/10}^9$ cells during the first 13 h and then declined to $763 \,\mu\text{M/h/10}^9$ cells. In contrast, in a similar HFB, Custer and Mullon (1998) reported lower O_2 consumption. The smaller porosity of the HF (0.2 μm vs. 0.5 μm) and the fact that they used cryopreserved hepatocytes instead of freshly isolated hepatocytes might explain this difference.

Kinetics of CAs in the Hepatocyte HFB

Our model was able to differentiate the behavior of the intracellular CA Gd-BOPTA from that of the extracellular CA Gd-DTPA (Fig. 7, Table I). The rapid and reversible evolution of SI obtained with Gd-DTPA can be explained by the fact that Gd-DTPA rapidly diffused from the ICS through the HF and filled the ECS of the bioreactor, i.e., the space around hepatocytes. During the washing, Gd-DTPA completely disappeared from the HFB. During the perfusion of the intracellular CA Gd-BOPTA, the same processes of diffusion and filling were observed, but with an additional phenomenon: Gd-BOPTA had an additional distribution space, as it could penetrate into hepatocytes. After washing, Gd-BOPTA was not completely washed from the bioreactor. A residual SI was observed, indicating that some Gd-BOPTA remained in hepatocytes or at least was released so slowly that the decrease was not detectable during the time period of the experiment. Because the SI returned to the baseline in control experiment (without hepatocytes), this residual SI could not be due to a possible Gd-BOPTA adsorption on the surface of the HF. ICP-AES analysis of the cell lysate confirmed the trapping of Gd-BOPTA in the hepatocytes. Moreover, by changing the concentration of Gd-BOPTA perfused, we showed that the residual SI measured increased with the concentration of CA.

In summary, we succeeded in developing an in vitro cellular model for the study of MR CAs, in which the trans-

port kinetics were investigated by MRI. The system was optimized to ensure a rapid diffusion of the CAs, nutrient, and O_2 to the hepatocytes. This cellular model offers a new tool to elucidate the transport mechanisms of hepatobiliary CAs. The detection of the CAs is obtained in the MR unit and the kinetics can be related to that observed in clinical exams. The use of this newly developed in vitro model could also be extended to transport studies with hepatocytes isolated from other species, such as humans, or from injured livers such as cirrhotic livers.

References

- Aime S, Cabella C, Colombatto S, Geninatti S, Gianolino E, Maggioni F. 2002. Insights into the use of paramagnetic Gd(III) complexes in MRmolecular imaging investigations. J Magn Reson Imag 16:394–406.
- Allen JW, Hassanein T, Bhatia SN. 2001. Advance in bioartificial liver devices. Hepatology 34:447–455.
- Colet J-M, Elst LV, Muller RN. 1998. Dynamic evaluation of the hepatic uptake of manganese-based MRI contrast agents: a 31P NMR study on the isolated perfused rat liver. J Magn Reson Imag 8:663–669.
- Custer LM, Mullon C. 1998. Oxygen delivery to and use by primary porcine hepatocytes in the HepaAssist 2000 system for extracorporeal treatment of patients in end-stage liver failure. Adv Exp Med Biol 454:261–271.
- De Haën C, Lorusso V, Tirone P. 1996. Hepatic transport of gadobenate dimeglumine in TR-rats. Acad Radiol 3:452–454.
- De Haën C, La Ferla R, Maggioni F. 1999. Gadobenate dimeglumine 0.5 M solution for injection (Multihence) as contrast agent for magnetic resonance imaging of the liver: mechanistic studies in animals. J Comput Assist Tomogr 23(Suppl. 1):S169–S179.
- Donoghue C, Brideau M, Newcomer P, Pangrle B, Dibiasio D, Walsh E, Moore S. 1992. Use of magnetic resonance imaging to analyse the performance of hollow-fiber bioreactors. Ann NY Acad Sci 665:285–300.
- Gallez B, Bacic G, Swartz HM. 1996a. Evidence for the dissociation of the hepatobiliary MRI contrast agent Mn-DPDP. Magn Reson Med 35: 14-19.
- Gallez B, Baudelet C, Adline J, Charbon V, Lambert DM. 1996b. The uptake of Mn-DPDP by hepatocytes is not mediated by the facilitated transport of pyridoxine. Magn Reson Imag 14:1191–1195.
- Gamcsik MP, Forder JR, Millis KK. 1995. A versatile oxygenator and perfusion system for magnetic resonances studies. Biotechnol Bioeng 49:348-354
- Gillies RJ, Scherer PG, Raghunand N, Okerlund LS, Martinez-Zaguilan R, Hesterberg L, Dale BE. 1991. Iteration of hybridoma growth and productivity in hollow fiber bioreactors using 31P NMR. Magn Reson Med 18:181–192.
- Giorgio TD, Moscioni AD, Rozga J, Demetriou AA. 1993. Mass transfer in a hollow fiber device used as a bioartificial liver. ASAIO J 39: 886–892.
- Greengard O, Federman M, Knox WE. 1972. Cytomorphology of developing rat liver and its application to enzyme differentiation. J Cell Biol 52:261–272.
- Gyngell ML. 1988. The application of steady-state free precession in rapid 2DFT NMR imaging: FAST and CE-FAST sequences. Magn Reson Imag 6:415–419.
- Hahn PF, Saini S. 1998. Liver-specific MR imaging contrast agents. Radiol Clin North Am 36:287–297.
- Hamilton RL, Berry MN, Williams MC, Severinghaus EM. 1974. A simple and inexpensive membrane "lung" for small organ perfusion. J Lipid Res 15:182–186.
- Hammer BE, Heath CA, Mirer SD, Belfort G. 1990. Quantitative flow measurement in bioreactors by nuclear magnetic resonance imaging. Biotechnology 8:327–330.
- Hammond AH, Fry JR. 1993. Maintenance of xenobiotic metabolism and toxicity in rat hepatocyte cultures after cell preservation at 4°. Biochem Pharmacol 46:333–335.

- Ivancevic MK, Zimine Y, Lazeyras F, Foxall D, Vallée JP. 2001. FAST sequences optimization for contrast media pharmacokinetic quantification in tissue. J Magn Reson Imag 14:771–778.
- Jackson LR, Trudel LJ, Fox JG, Lipman NS. 1996. Evaluation of hollow fiber bioreactors as an alternative to murine ascites production for small scale monoclonal antibody production. J Immunol Methods 189: 217–231.
- Knazek RA, Skyler JS. 1976. Secretion of human prolactin in vitro. Proc Soc Exp Biol Med 151:561–564.
- Knazek RA, Gullino PM, Kohler PO, Dedrick RL. 1972. Cell culture on artificial capillaries: an approach to tissue growth in vitro. Science 178: 65–67.
- Kreutz FT, Jafarin A, Biggs DF, Suresh MR. 1997. Production of highly pure monoclonal antibodies without purification using hollow fiber bioreactor. Hybridoma 16:485–486.
- Liu JJ, Chen BS, Tsai TF, Wu YJ, Pang VF, Hsieh A, Hsieh JH, Chang TH. 1991. Long term and large scale cultivation of human hepatoma Hep G2 cells in hollow fiber bioreactor. Cytotechnology 5:129–139.
- Lorusso V, Arbughi T, Tirone P, De Haën C. 1999. Pharmacokinetics and tissue distribution in animals of gadobenate ion, the magnetic resonance imaging contrast enhancing component of gadobenate dimeglumine 0.5 M solution for injection (MultiHance). J Comput Assist Tomogr 23(Suppl. 1):181–194.
- Macdonald JM, Grillo M, Schmidlin O, Tajiri DT, James TL. 1998. NMR spectroscopy and MRI investigation of a potential bioartificial liver. NMR Biomed 11:55-66.
- Mamprin ME, Rodriguez JV, Guibert EE. 1995. Importance of pH in resuspension media on viability of hepatocytes preserved in University of Wisconsin solution. Cell Transplant 4:269–274.
- Mizutani T. 1982. Adsorption of some antibiotics and other drugs on silicone-coated glass surfaces. J Pharm Pharmacol 34:608–609.
- Nyberg SL, Remmel RP, Mann HJ, Peshwa MV, Hu W-S, Cerra FB. 1994.Primary hepatocytes outperform Hep G2 cells as the source of biotransformation functions in a bioartificial liver. Ann Surg 220:59–67.
- Olinga P, Merema M, Slooff MJH, Meijer DKF, Groothuis GMM. 1997. Influence of 48 hours cold storage in University of Wisconsin organ preservation solution on metabolic capacity of rat hepatocytes. J Hepatol 27:738–743.
- Osuga T, Obata T, Ikehira H, Tanada S, Sasaki Y, Naito H. 1998. Dialysate pressure isobars in a hollow-fiber dialyzer determined from magnetic resonance imaging and numerical simulation of dialysate flow. Artif Organs 22:907–909.
- Pascolo L, Cupelli F, Anelli PL, Lorusso V, Visigalli M, Uggeri F, Tiribelli C. 1999. Molecular mechanisms for the hepatic uptake of magnetic resonance imaging contrast agents. Biochem Biophys Res Commun 257:746-752.
- Pascolo L, Petrovic S, Cupelli F, Bruschi CV, Anelli PL, Lorusso V, Visigalli M, Uggeri F, Tiribelli C. 2001. ABC protein transport of MRI contrast agents in canalicular rat liver plasma vesicles and yeast vacuoles. Biochem Biophys Res Commun 282:60–66.
- Patzer JF II. 2001. Advances in bioartificial liver assist devices. Ann NY Acad Sci 944:320–333.
- Potter K, Butler JJ, Adams C, Fishbein KW, Mcfarland EW, Horton WE, Spencer RGS. 1998. Cartilage formation in a hollow fiber bioreactor studied by proton magnetic resonance microscopy. Matrix Biol 17: 513-523.
- Reimer P, Bader A, Weissleder R. 1998. Preclinical assessment of hepatocyte-targeted MR contrast agents in stable human cell cultures. J Magn Reson Imag 8:687–689.
- Rosen DA, Rosen KR, Silvasi DL. 1990. In vitro variability in fentanyl absorption by different membrane oxygenators. J Cardiothoracic Anesth 4:332–335.
- Rotem A, Toner M, Tompkins RG, Yarmush ML. 1992. Oxygen uptake rates in cultures rat hepatocytes. Biotechnol Bioeng 40:1286–1291.
- Rozga J, Williams F, Ro M-S, Neuzil DF, Giorgio TD, Backfisch G, Moscioni D, Hakim R, Demetriou AA. 1993. Development of a bioartificial liver: properties and function of a hollow-fiber module inoculated with liver cells. Hepatology 17:258–265.

- Sandker GW, Weert B, Slooff MJH, Groothuis GMM. 1990. Preservation of isolated rat and human hepatocytes in UW solution. Transplant Proc 22:2204–2205.
- Sandker GW, Slooff MJH, Groothuis GMM. 1992. Drug transport, viability and morphology of isolated rat hepatocytes preserved for 24 hours in University of Wisconsin solution. Biochem Pharmacol 43:1479 – 1485.
- Sasse D, Spornitz UM, Maly IP. 1992. Liver architecture. Enzyme 46:8–32.
- Schmalbrock P, Hines JV, Lee S-M, Ammar GM, Kwok EW-C. 2001. T1 measurement in cell cultures: a new tool for characterizing contrast agents at 1.5T. J Magn Reson Imag 14:636–648.
- Schulze E, Ferrucci JT, Poss K, Lapointe L, Bogdanova A, Weissleder R. 1995. Cellular uptake and trafficking of a prototype magnetic iron oxide label in vitro. Invest Radiol 30:604-610.
- Seglen O. 1976. Preparation of isolated rat liver cells. In: Prescott DM, editor. Methods in cell biology. New York: Academic Press. p 29–83.
- Semelka RC, Helmberger TKG. 2001. Contrast agents for MR imaging of the liver. Radiology 28:27–38.

- Taylor HM, Ros PR. 1998. Hepatic imaging. Radiol Clin North Am 36:237–245.
- Tharakan JP. 1986. Operation and pressure distribution of immobilized cell hollow fiber bioreactors. Biotechnol Bioeng 28:1064–1071.
- Tze WJ, Tai J, Wong FC, Davis HR. 1980. Studies with implantable artificial capillary units containing rat islets on diabetic dogs. Diabetologica 19:541–545.
- Van Montfoort JE, Stieger B, Meijer DKF, Weinmann H-J, Meier PJ, Fattinger KE. 1999. Hepatic uptake of the magnetic resonance imaging contrast agent gadoxetate by the organic anion transporting polypeptide Oatp1. J Pharmacol Exp Ther 290:153–157.
- Weibel ER, Staubli W, Gnagi HR, Hess FA. 1969. Correlated morphometric and biochemical studies on the liver cell. J Cell Biol 42: 68-91
- Zhang J, Parker DL, Leypoldt JK. 1995. Flow distributions in hollow fiber hemodialyzers using magnetic resonance Fourier velocity imaging. ASAIO J 41:678–682.